Energy Transfer between Inorganic Perovskite Nanocrystals

de Weerd, C.; Gomez, L.; Zhang, H.; Buma, W.J.; Nedelcu, G.; Kovalenko, M.V.; Gregorkiewicz, T.

DOI
10.1021/acs.jpcc.6b04768

Publication date
2016

Document Version
Final published version

Published in
The Journal of Physical Chemistry. C

THE JOURNAL OF PHYSICAL CHEMISTRY C

Article

pubs.acs.org/JPCC

Energy Transfer between Inorganic Perovskite Nanocrystals

Chris de Weerd,*[,†] Leyre Gomez,*[,†] Hong Zhang,[‡] Wybren J. Buma,[‡] Georgian Nedelcu,[§,∥] Maksym V. Kovalenko,[§,∥] and Tom Gregorkiewicz[†]

[†]Institute of Physics and [‡]Van't Hoff Institute for Molecular Sciences, University of Amsterdam, Science Park 904, 1098 XH Amsterdam, The Netherlands

[§]Institute of Inorganic Chemistry, Department of Chemistry and Applied Bioscience, ETH Zürich, CH-8093 Zürich, Switzerland

[∥]Laboratory for Thin Films and Photovoltaics, Empa − Swiss Federal Laboratories for Materials Science and Technology, CH-8600 Dübendorf, Switzerland

Supporting Information

ABSTRACT: Cesium lead halide nanocrystals are a new attractive material for optoelectronic applications since they combine the advantageous properties of perovskites and quantum dots. For future applications in optoelectronics and photovoltaics, an efficient energy and/or carrier exchange is a necessary condition. Here, we explicitly demonstrate nonradiative energy transfer for colloidal $CsPbBr_3$ nanocrystals. Using time-resolved optical characterization of purposefully prepared batches of nanocrystals with different sizes, we identify the energy transfer which can be driven by the concentration gradient of excited nanocrystals as well as by the bandgap energy difference. The latter process moves the energy from smaller to larger nanocrystals and opens a possibility of directional streaming of the excitation energy in these materials. The observed energy transfer is enabled in the colloids by proximity of individual nanocrystals due to clustering.

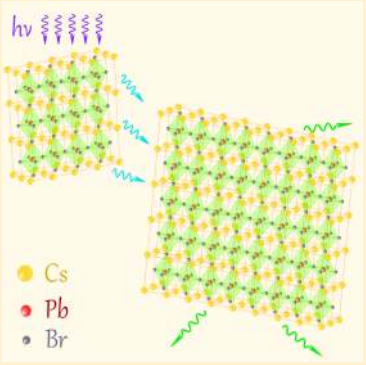

1. INTRODUCTION

Metal halide semiconductors with perovskite structure have attracted much interest in the past years due to their high emission efficiencies and low production costs, making them attractive for photovoltaic and optoelectronic applications.[1,2] Most of the progress in this research field has been focused on hybrid organic−inorganic perovskites[3,4] (e.g., $CH_3CH_3PbI_3$, $CH_3NH_3PbI_3$, etc.) as a solid state material supported on a substrate, with grain sizes outside of the nanoscale.[5−7] On the other hand, colloidal semiconductor nanocrystals (NCs)[8,9] (e.g., CdSe, CdTe, PbS, etc.) have also been widely studied as optoelectronic materials because their optical properties are enhanced by quantum-confinement effects.[10−12] The advantages of using semiconductor perovskites and NCs are combined in the colloidal inorganic cesium lead halide NCs ($CsPbX_3$, X = Cl, Br, and I) with cubic perovskite structure. They were first synthesized by Protesescu et al.,[13] and their photoluminescence (PL) is characterized by narrow emission bands and high quantum yields (QYs) of 50−90%. The novelty of this material has driven many investigations during the past year, for instance studies of air stability,[14,15] optical properties,[16,17] and lasing.[18−20] To design efficient optoelectronic devices based on semiconductor NCs,[21,22] the interaction between individual NCs needs to be evaluated and possibly engineered. In particular, for photovoltaic cells, an exciton generated upon photon absorption needs to be either separated into an electron and a hole pair and the free carriers are transported toward the respective electrodes (semiconductor cells)[23] or moved toward an interface and be split there (polymer cells).[24] In general, there are three possible mechanisms of exciton transfer:[25] cascade energy transfer (involving emission and subsequent reabsorption of a photon), Dexter transfer (involving electron exchange interactions), and Förster resonance energy transfer (FRET), mediated by Coulomb interactions between a donor and acceptor. Here, we explore the energy transfer (ET) between NCs, from a donor to an acceptor with a lower bandgap energy. ET between direct bandgap semiconductor NCs is typically described by FRET,[26] which depends on the spectral overlap of donor emission and acceptor absorption, and the donor−acceptor Coulomb coupling, determined by the distance between them. ET in closed-packed ensembles of NCs of direct bandgap semiconductors (CdSe, CdTe, PbS, InP, etc.) has been demonstrated in the past by means of changes in the PL spectra and lifetimes.[27−30] Also, the energy exchange between NCs of silicon, the most widely used material for photovoltaics and electronics, has been conclusively established.[31,32] In hybrid perovskite-based solar cells, energy exchange has just been observed between perovskite films and layers of organic electron and hole acceptors[33,34] and a so-called "dots-in-a-matrix" using PbS NCs.[35] Accordingly, also exciton transfer between perovskite NCs could be expected but has not been shown until now. To the contrary, a recent study on perovskite NC films revealed no evidence of ET.[36] While this negative

Received: May 11, 2016
Revised: May 26, 2016
Published: May 26, 2016

DOI: 10.1021/acs.jpcc.6b04768
J. Phys. Chem. C 2016, 120, 13310−13315

result was tentatively explained by large sizes of the investigated materials, the urgent need for further research appeared.

In this work, we investigate ET between cesium lead bromide ($CsPbBr_3$) all-inorganic NCs with perovskite structure in colloidal state and provide explicit and conclusive evidence of effective ET proceeding from small to large NCs. We show that the ET process in the investigated colloids is enabled by clustering which brings the NCs in direct contact.

2. EXPERIMENTAL SECTION

Materials. Cesium carbonate (Cs_2CO_3, 99.9%, Sigma-Aldrich), octadecene (ODE, 90%, Sigma-Aldrich), oleic acid (OA, 90%, Sigma-Aldrich), oleylamine (OLA, 80−90%, Acros), lead(II) bromide ($PbBr_2$, 98%, Sigma-Aldrich), and toluene (ACS reagent, ≥99.5%, Sigma-Aldrich) were used with no further purification, except for the drying period reported in the synthesis procedure.

Synthesis. Cesium lead bromide perovskites ($CsPbBr_3$) were synthesized as described by Protesescu et al.[13] Summarizing, 5 mL of ODE and 70 mg of $PbBr_2$ were dried for 1 h at 120 °C under a N_2 atmosphere. After water removal, 0.5 mL of dried OLA and 0.5 mL of dried OA were added to the reaction flask, and the temperature was raised up to the desired value. After complete solvation of the $PbBr_2$ salt, 0.4 mL of a previously synthesized Cs-oleate solution in ODE was injected. A few seconds later, the NC solution was quickly cooled down with an ice bath. The product was purified by centrifugation and redispersion in toluene. The perovskite synthesis was carried out at two different temperatures, yielding different NC sizes as described in the literature.[13] The samples that were studied have a concentration of 0.2 mg/mL, as determined from the dry weight.

Characterization. The optical density of the investigated colloids was measured in a LAMBDA 950 UV/vis/NIR spectrophotometer (PerkinElmer). A combination of a tungsten−halogen and deuterium lamp is used together with a PMT and Peltier cooled PbS detector to provide a detection range of E_{det} = 5.6−0.4 eV. The sample and solvent measurements have been performed separately and afterward subtracted from each other. The PL has been studied under excitation by a Nd:YAG-pumped optical parametric oscillator (OPO) (repetition rate $f \approx 100$ Hz, pulse width Δt = 5 ns, excitation energy E_{exc} = 2.88 eV) and collected under a right-angle geometry and subsequently detected by a CCD (Hamamatsu S10141-1108S) coupled to a spectrometer (Solar, M266) or a PMT (Hamamatsu R9110). The spectra were corrected for the spectral sensitivity of the setup. The samples can also be placed in an integrating sphere to determine the PL quantum yield, using a 150 W xenon lamp coupled to a spectrometer (Solar, MSA-130) as an excitation source. The PL emission and excitation light are scattered diffusively in the integrating sphere and are detected by the CCD. See also ref 46 for a full description of the adopted method. The picosecond PL dynamics have been measured using the frequency-doubled output of a tunable Ti:sapphire laser system (Chameleon Ultra, Coherent), providing 140 fs pulses at E_{exc} = 2.88 eV. A pulse picker has been employed to reduce the repetition rate from 80 to 8 MHz. The PL emission has been detected using a monochromator (Newport CS260-02) coupled to a PMT (Hamamatsu) providing a total detection range of E_{det} = 6−1.6 eV. The overall instrument response function (IRF) is 20−25 ps (fwhm) as measured from a dilute scattering solution (Ludox) at the excitation wavelength. All measurements have been performed at room temperature.

3. RESULTS AND DISCUSSION

The colloidal synthesis yields near-monodisperse $CsPbBr_3$ NCs with a cubic perovskite structure whose size, and therefore PL emission energy, can be tuned between approximately 2.3 and 2.7 eV by controlling the temperature at which the synthesis is performed.[13] Figure 1 shows the optical characterization (see also Figure S1 in the Supporting Information) and TEM images for the materials used in this study (samples A and B). The PL bands (Figure 1a) centered at 2.43 and 2.36 eV for samples A and B with full widths at half-maximum of 0.1 and 0.089 eV, respectively, show a small Stokes shift from their corresponding absorption spectra that exhibit a clear excitonic peak at the onset. The inset shows the samples under UV illumination indicating that they are similarly bright to the eye; a minor difference in color can hardly be distinguished. We have determined a PL quantum yield of ∼90% and ∼30% for samples A and B, respectively. The TEM images with their corresponding histograms (Figures 1b−e) confirm the formation of cubic NCs with an average edge size of 8.4 ± 1.4 and 18.3 ± 2.8 nm for samples A and B, respectively. We note that synthesis at a higher temperature (sample B) leads to a larger size distribution of the NCs and an occasional shape deformation. A similar PL line width of both samples A and B (Figure 1a) in spite of the significantly broader size distribution of sample B (Figures 1c,e) is the first indication of a possible excitation flow into a smaller subensemble of emitters.

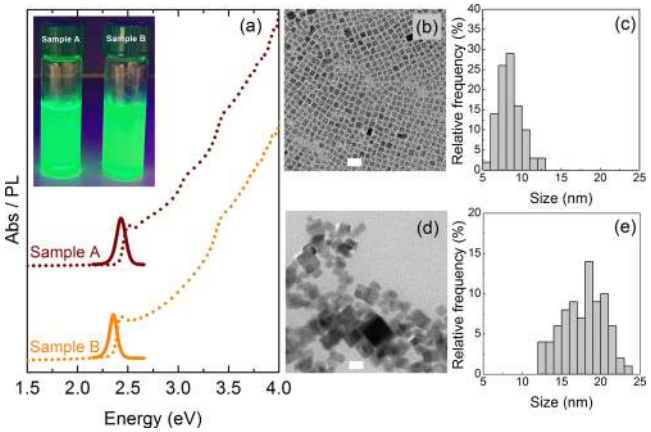

Figure 1. (a) Absorption and photoluminescence spectra of samples A and B. The inset shows the samples under UV illumination (365 nm). TEM images (scale bar corresponds to 20 nm) with the corresponding histograms of samples A and B indicating cubic nanocrystals with an edge size of 8.4 ± 1.4 nm (b, c) and 18.3 ± 2.8 nm (d, e), respectively.

In case that the energy transfer takes place, one can expect that the ensemble emission spectrum will be reduced on the high-energy side, and part of this intensity loss will reappear at a lower energy, since transfer only occurs from smaller to larger NCs. Such a spectral deformation can be induced by reabsorption of higher energy photons or by direct (photonless) ET between adjacent NCs; in either case, the measured PL band will be red-shifted and will not have the usual Gaussian distribution of photon energies (resulting from the Gaussian distribution of NC sizes). Since the optical characteristics of the investigated samples are known, the PL spectrum can be easily corrected for reabsorption using the Lambert−Beer law:[37,38]

DOI: 10.1021/acs.jpcc.6b04768
J. Phys. Chem. C 2016, 120, 13310−13315

$$\log \frac{I^0(\lambda)}{I(\lambda)} = \mathrm{OD}$$

where $I^0(\lambda)$ is the reabsorption free emission, $I(\lambda)$ is the measured emission, and OD is the optical density determined from the steady-state absorption. Figure 2 shows the PL

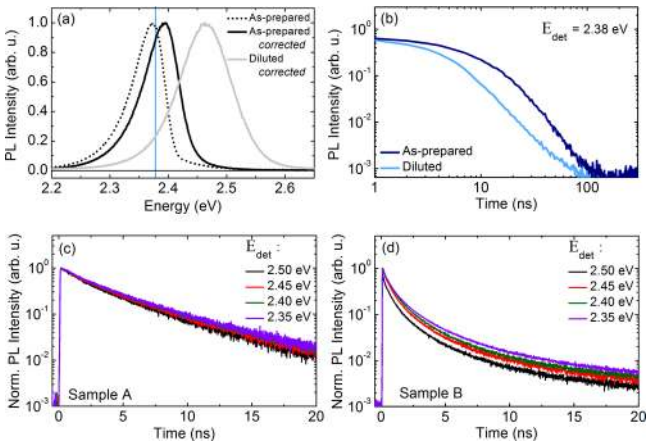

Figure 2. (a) Normalized PL spectrum for sample A as-prepared (black) and sufficiently diluted (gray), corrected for reabsorption. Plotted in the same graph is the uncorrected spectrum of the as-prepared sample to demonstrate the effect of reabsorption on the emission spectrum. The solid line indicates where the time-resolved signal is detected. (b) PL decay detected at 2.38 eV for the respective samples. (c, d) Normalized time-resolved PL signal recorded at different detection energies for samples A and B, respectively.

spectrum of sample A as measured (black, dotted) and corrected for reabsorption (black); as can be seen, the corrected PL spectrum shifts to the blue but remains asymmetric. On the other hand, being strongly distance-dependent, FRET can be fully eliminated by sufficient dilution. Indeed, we have observed that with increasing dilution the PL spectrum continued to blue-shift until it stabilized upon reaching a sufficiently low NC concentration; see the gray spectrum in Figure 2. We note that upon sufficient dilution, the PL spectrum attains the Gaussian shape, as expected. We conclude that the gray spectrum represents the true PL of sample A, free from any effects of ET; the fact that it is not identical with the corrected one for reabsorption (black) indicates the presence of ET. In the case of molecules, when the donor can be selectively excited, the ET can be directly monitored by investigating the PL dynamics,[30] by the time-dependent rise of the acceptor emission. In the case of ET between NCs, it is not possible to excite the donor without simultaneous excitation of the acceptor. However, the lengthening of the PL lifetime as a result of multiple ET events taking place prior to radiative recombination should appear. We remark that in principle the lengthening of the PL lifetime can also appear due to a change in the dielectric constant of the sample as the NC density increases.[39,40] However, due to the low volume fraction (of the order of 10^{-6}) of the colloids investigated in this study, this effect can be neglected.[41] Figure 2b shows the time-resolved PL signal at 2.38 eV for sample A before and after dilution, i.e., with the highest and the lowest NC density. As can be seen, the PL lifetime increases with NC density. This is readily explained by a higher probability of ET as the NCs are closer together, with the multiple ET events lengthening the lifetime. The increase of the lifetime is the most significant on the low-energy side since the transfer takes place from smaller (donors) to larger (acceptors) NCs (see Figure S2). To further investigate the possible PL dynamic change by ET, we measured the time-resolved PL signal at different detection energies. This is shown in Figures 2c and 2d for samples A and B, respectively. As can be seen, they both show a gradual increase of the PL lifetime toward lower energies, consistent with ET toward larger NCs.

A measure for the ET can be determined by comparing the emission of the as-prepared (ET takes place) and diluted (no ET takes place) samples. This is done by fitting both spectra using a number of Gaussian subcomponents centered at arbitrary chosen energies (Figures 3a,b). Upon ET, part of the

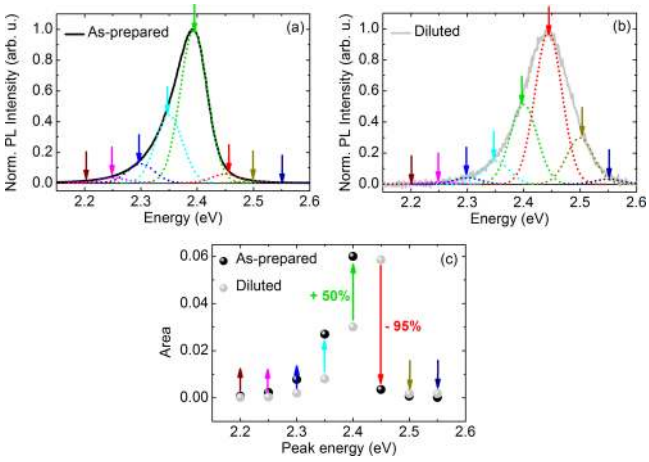

Figure 3. PL spectra (corrected for reabsorption) of sample A as-prepared (a, black) and diluted (b, gray). The spectra are fitted using a number of Gaussian subcomponents (dotted lines) with the same peak energy for both samples (indicated by the colored arrows). (c) For each component the increase and decrease of the area under the curve are given. For the chosen components, we find a maximum increase of 50% at 2.4 eV and a decrease of 95% at 2.45 eV.

emission on the high-energy side will decrease and subsequently reappear on the low-energy side. In this way, the area under each respective Gaussian (with the same peak energy) can be compared, providing a measure for the (maximum) amount of transferred excitons. In addition, the PL spectrum of the as-prepared sample can be fitted with a single Gaussian distribution where there remains a large discrepancy on the low-energy side (see Figure S3). The difference in integrated area under both curves is a measure for the minimum amount of carriers that are transferred. We find a maximum of 50% increase at 2.4 eV and a minimum of 35% transfer from the donor to the acceptor side.

In order to prove the presence of ET in the investigated material, we performed a dedicated experiment. For that purpose we mixed samples A and B at different ratios (A:B volume ratio equal to 4:1, 1:1, and 1:4) and subsequently recorded the PL spectra and decay dynamics of the mixed colloids. In order to preliminarily reduce the effects of reabsorption, samples A and B have been diluted prior to mixing such that the correction for reabsorption does not induce a considerable change of the spectrum. We note that ET can still take place since upon even further dilution, a considerable blue-shift of the PL spectrum was observed, as ET can be eliminated by reducing the concentration (as previously explained in Figure 2a). Nonetheless, all PL spectra

DOI: 10.1021/acs.jpcc.6b04768
J. Phys. Chem. C 2016, 120, 13310−13315

are corrected for a possible remaining reabsorption. Figure 4a shows the PL spectra of the samples A and B and their different

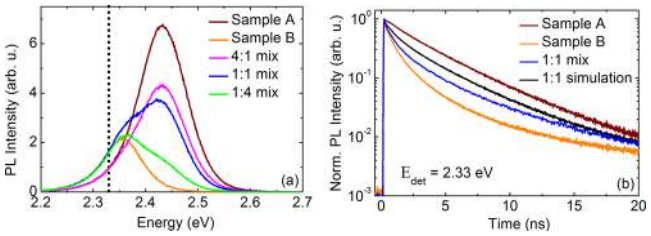

Figure 4. (a) PL spectra (corrected for reabsorption) of samples A (brown) and B (orange) and of the mixed compositions with A:B ratios of 4:1 (pink), 1:1 (blue), and 1:4 (green). (b) Normalized time-resolved PL signal recorded at 2.33 eV for samples A and B as well as the 1:1 mixed sample and the simulated decay.

mixtures. We clearly observe a shift of the PL spectrum, with the maximum changing continuously from that of the small NCs (sample A) to that of the larger ones (sample B) while an increasing fraction of small NCs is gradually substituted by the large ones. Furthermore, for the 1:1 and 1:4 mixing ratios (blue and green spectra), a shoulder appears, being consistent with the two different sizes present in the sample. Figure 4b shows the time-resolved PL signal for samples A and B and the 1:1 mix (brown, orange, blue), detected at 2.39 eV. Included in the same graph is the simulated decay trace of the 1:1 mixed sample. This is obtained from simply summing the two experimentally obtained PL decay signals of samples A and B and subsequent dividing by two. It can be clearly seen that the simulated and the experimentally obtained PL decays are not identical. This indicates that an additional transfer processes is enabled upon mixing.

The ET can be further analyzed by comparing the experimentally measured PL spectra of the mixed samples and their simulated spectra. The latter are obtained, similarly as shown in Figure 4b, from adding the measured PL spectra of samples A and B according to their mixing ratios. Figure 5

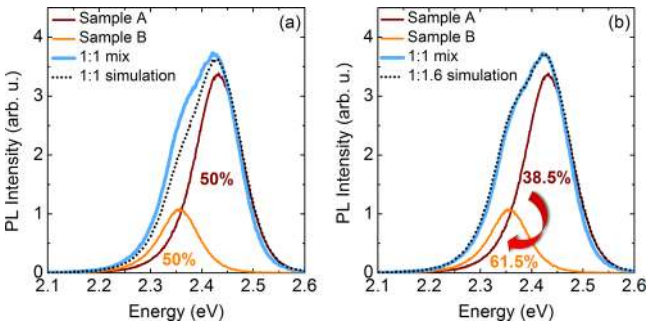

Figure 5. (a) PL spectra of sample A and B and the 1:1 mixed colloid. The dotted lines represent the simulated PL spectra of the mixed sample using nominal (a) and scaled (b) composition. All PL spectra have been corrected for reabsorption.

shows the PL spectra of samples A and B and the 1:1 mixed colloid (solid lines). The dotted lines indicate the simulated spectra using nominal (Figure 5a) and scaled (Figure 5b) 1:1 composition. A considerable ET from the donors to the acceptors has to be assumed in order to fit the experimental data: the contribution of the large NCs to the emission had to be enhanced by a factor of 1.6. This is the result of donors transferring their energy instead of emitting. For the 4:1 and 1:4 mixed colloidal suspensions, similar discrepancies between the experimentally measured and simulated PL spectra are observed (see Figure S4).

The spectral and temporal changes as shown in Figures 4 and 5 upon the introduction of acceptors, which cannot be modeled and correctly predicted using equal contributions of the donors and acceptors, are consistent with the presence of ET.[42] Figure 5b shows a considerable transfer from the donors to the acceptors. For completeness we note that an alternative explanation of spectral modification by ligand exchange between NCs of samples A and B upon mixing[41] can be disregarded since, as discussed, evidence of ET has also been obtained for both samples separately, before mixing. However, the dynamic interaction of the ligands with the NC surface can be responsible for clustering of the NCs with time, which, in turn, enables the ET.[41]

In the past investigations, ET between semiconductor NCs has mostly been observed in close-packed solids and seldom in dispersed colloids.[27,30,43−45] In order to further investigate the ET in colloidal dispersions reported here, the NCs aggregation was examined. The TEM results revealed the presence of NC clustering (see Figure S5). Although it is known that these NCs self-assemble upon drying, it is consistent with the observations of precipitated NCs, and it also explains the spectral modifications upon time. An enhancement of ET as the colloids are allowed to settle for a few hours after mixing is observed (see Figure S6). Upon clustering, the contribution of the acceptors emission to the PL spectrum significantly increases. This indicates ET between NCs, but could alternatively be interpreted being due to sintering and formation of bigger chunks of material. However, since the clustering involves a large amount of NCs, the PL maximum would red-shift to the bulk value, which is not the case.

4. CONCLUSIONS

We have established the presence of effective ET between inorganic perovskite $CsPbBr_3$ NCs in colloidal state, driven by concentration and energy gradients. This opens new insights for application of perovskite NCs where the ET can be engineered toward a specific goal.

■ ASSOCIATED CONTENT

Supporting Information

The Supporting Information is available free of charge on the ACS Publications website at DOI: 10.1021/acs.jpcc.6b04768.

Absorption spectra of all considered samples with and without correction for the solvent absorption and the corresponding PL spectra (Figure S1); PL lifetimes at different detection energies for sample A (Figure S2); comparison of the normalized PL spectra measured and simulated (Figure S3); fitting of the normalized PL spectra of sample A corrected for reabsorption (Figure S4); TEM image of NCs aggregation (Figure S5); normalized PL spectra for the different mixed samples (Figure S6) (PDF)

■ AUTHOR INFORMATION

Corresponding Authors

*(C.d.W.) Tel (+31) 205255644, e-mail c.deweerd@uva.nl.

*(L.G.) Tel (+31) 205256339, e-mail l.gomeznavascues@uva.nl.

DOI: 10.1021/acs.jpcc.6b04768
J. Phys. Chem. C 2016, 120, 13310−13315

Author Contributions

C.d.W. and L.G. contributed equally. C.d.W., L.G., and T.G. conceived the project and designed the experiments; L.G. and G.N. prepared the samples; C.d.W. performed the spectroscopy measurements; G.N. and M.V.K. performed the TEM measurements; C.d.W. analyzed the data; C.d.W., L.G., and T.G. interpreted the data and cowrote the manuscript; H.Z. and W.J.B. facilitated the ultrafast time-resolved experiments; H.Z., W.J.B., G.N., and M.V.K. edited the manuscript. The manuscript was written through contributions of all authors. All authors have given approval to the final version of the manuscript.

Notes

The authors declare no competing financial interest.

■ ACKNOWLEDGMENTS

This work was financially supported by Stichting voor Fundamenteel Onderzoek der Materie (FOM) and by Technologiestichting STW, The Netherlands.

■ REFERENCES

(1) Bisquert, J. The Swift Surge of Perovskite Photovoltaics. *J. Phys. Chem. Lett.* **2013**, *4*, 2597−2598.
(2) Kazim, S.; Nazeeruddin, M. K.; Gratzel, M.; Ahmad, S. Perovskite as Light Harvester: A Game Changer in Photovoltaics. *Angew. Chem., Int. Ed.* **2014**, *53*, 2812−2824.
(3) Sum, T. C.; Mathews, N. Advancements in Perovskite Solar Cells: Photophysics Behind the Photovoltaics. *Energy Environ. Sci.* **2014**, *7*, 2518−2534.
(4) Filippetti, A.; Mattoni, A. Hybrid Perovskites for Photovoltaics: Insights from First Principles. *Phys. Rev. B: Condens. Matter Mater. Phys.* **2014**, *89*, 125203-1−125203-8.
(5) Brivio, F.; Walker, A. B.; Walsh, A. Structural and Electronic Properties of Hybrid Perovskites for High-Efficiency Thin-Film Photovoltaics from First-Principles. *APL Mater.* **2013**, *1*, 042111-1−042111-5.
(6) Stranks, S. D.; Nayak, P. K.; Zhang, W.; Stergiopoulos, T.; Snaith, H. J. Formation of Thin Films of Organic−Inorganic Perovskites for High-Efficiency Solar Cells. *Angew. Chem., Int. Ed.* **2015**, *54*, 3240−3248.
(7) Nie, W.; Tsai, H.; Asadpour, R.; Blancon, J. C.; Neukirch, A.; Gupta, G.; Crochet, J. J.; Chhowalla, M.; Tretiak, S.; Alam, M. A.; et al. High-Efficiency Solution-Processed Perovskite Solar Cells with Millimeter-Scale Grains. *Science* **2015**, *347* (6221), 522−525.
(8) Bawendi, M. G.; Steigerwald, M. L.; Brus, L. E. The Quantum Mechanics of Larger Semiconductor Clusters ("Quantum Dots"). *Annu. Rev. Phys. Chem.* **1990**, *41*, 477−96.
(9) Alivisatos, A. P. Semiconductor Clusters, Nanocrystals, and Quantum Dots. *Science* **1996**, *271*, 933−937.
(10) Kramer, I. J.; Sargent, E. H. Colloidal Quantum Dot Photovoltaics: A Path Forward. *ACS Nano* **2011**, *5* (11), 8506−8514.
(11) Sargent, E. H. Colloidal Quantum Dot Solar Cells. *Nat. Photonics* **2012**, *6*, 133−135.
(12) Chuang, C. H. M.; Brown, P. R.; Bulovic, V.; Bawendi, M. G. Improved Performance and Stability in Quantum Dot Solar Cells Through Band Alignment Engineering. *Nat. Mater.* **2014**, *13*, 796−801.
(13) Protesescu, L.; Yakunin, S.; Bodnarchuk, M. I.; Krieg, F.; Caputo, R.; Hendon, C. H.; Yang, R. X.; Walsh, A.; Kovalenko, M. V. Nanocrystals of Cesium Lead Halide Perovskites ($CsPbX_3$, X = Cl, Br, and I): Novel Optoelectronic Materials Showing Bright Emission with Wide Color Gamut. *Nano Lett.* **2015**, *15*, 3692−3696.
(14) Pan, J.; Sarmah, S. P.; Murali, B.; Dursum, I.; Peng, W.; Parida, M. R.; Liu, J.; Sinatra, L.; Alyami, N.; Zhao, C.; et al. Air-Stable Surface-Passivated Perovskite Quantum Dots for Ultra-Robust, Single- and Two-Photon-Induced Amplified Spontaneous Emission. *J. Phys. Chem. Lett.* **2015**, *6*, 5027−5033.
(15) Palazon, F.; Akkerman, Q. A.; Prato, M.; Manna, L. X-ray Lithography on Perovskite Nanocrystals Films: From Patterning with Anion-Exchange Reactions to Enhanced Stability in Air and Water. *ACS Nano* **2016**, *10*, 1224−1230.
(16) Nedelcu, G.; Protesescu, L.; Yakunin, S.; Bodnarchuk, M. I.; Grotevent, M. J.; Kovalenko, M. V. Fast Anion-Exchange in Highly Luminescent Nanocrystals of Cesium Lead Halide Perovskites ($CsPbX_3$, X = Cl, Br, I). *Nano Lett.* **2015**, *15*, 5635−5640.
(17) Akkerman, Q. A.; D'Innocenzo, V.; Accornero, S.; Scarpellini, A.; Petrozza, A.; Prato, M.; Manna, L. Tuning the Optical Properties of Cesium Lead Halide Perovskite Nanocrystals by Anion Exchange Reactions. *J. Am. Chem. Soc.* **2015**, *137*, 10276−10281.
(18) Yakunin, S.; Protesescu, L.; Krieg, F.; Bodnarchuk, M. I.; Nedelcu, G.; Humer, M.; de Luca, G.; Fiebig, M.; Heiss, W.; Kovalenko, M. V. Low-Threshold Amplified Spontaneous Emission and Lasing from Colloidal Nanocrystals of Cesium Lead Halide Perovskites. *Nat. Commun.* **2015**, *6*, 8056−8064.
(19) Wang, Y.; Li, X.; Song, J.; Xiao, L.; Zeng, H.; Sun, H. All-Inorganic Colloidal Perovskite Quantum Dots: A New Class of Lasing Materials with Favorable Characteristics. *Adv. Mater.* **2015**, *27*, 7101−7108.
(20) Wang, Y.; Li, X.; Zhao, X.; Xiao, L.; Zeng, H.; Sun, H. Nonlinear Absorption and Low-Threshold Multi-Photon Pumped Stimulated Emission from All-Inorganic Perovskite Nanocrystals. *Nano Lett.* **2016**, *16*, 448−453.
(21) Kamat, P. V. Quantum Dot Solar Cell: Semiconductor Nanocrystals as Light Harvesters. *J. Phys. Chem. C* **2008**, *112*, 18737−18753.
(22) Nozik, A. J. Nanoscience and Nanostructures for Photovoltaics and Solar Fuels. *Nano Lett.* **2010**, *10*, 2735−2741.
(23) Akselrod, G. M.; Prins, F.; Poulokakos, L. V.; Lee, E. M. Y.; Weidman, M. C.; Mork, A. J.; Willard, A. P.; Bulović, V.; Tisdale, W. A. Subdiffusive Exciton Transport in Quantum Dot Solids. *Nano Lett.* **2014**, *14*, 3556−3562.
(24) Albrecht, S.; Vandewal, K.; Tumbleston, J. R.; Fischer, F. S. U.; Douglas, J. D.; Fréchet, M. J.; Ludwigs, S.; Ade, H.; Salleo, A.; Neher, D. On the Efficiency of Charge Transfer State Splitting in Polymer: Fullerene Solar Cells. *Adv. Mater.* **2014**, *26*, 2533−2539.
(25) Menke, S. M.; Holmes, R. J. Exciton Diffusion in Organic Photovoltaic Cells. *Energy Environ. Sci.* **2014**, *7*, 499−512.
(26) Allan, G.; Delerue, C. Energy Transfer Between Semiconductor Nanocrystals: Validity of Förster's Theory. *Phys. Rev. B: Condens. Matter Mater. Phys.* **2007**, *75*, 195311-1−195311-8.
(27) Kagan, C. R.; Murray, C. B.; Nirmal, M.; Bawendi, M. G. Electronic Energy Transfer in CdSe Quantum Dot Solids. *Phys. Rev. Lett.* **1996**, *76*, 1517−1520.
(28) Micic, O. I.; Jones, K. M.; Cahill, A.; Nozik, A. J. Optical, Electronic, and Structural Properties of Uncoupled and Close-Packed Arrays of InP Quantum Dots. *J. Phys. Chem. B* **1998**, *102*, 9791−9796.
(29) Lunz, M.; Bradley, A. L.; Chen, W. Y.; Gun'ko, Y. K. Förster Resonant Energy Transfer in Quantum Dot Layers. *Superlattices Microstruct.* **2010**, *47*, 98−102.
(30) Crooker, S. A.; Hollingsworth, J. A.; Tretiak, S.; Klimov, V. I. Spectrally Resolved Dynamics of Energy Transfer in Quantum-Dot Assemblies: Towards Engineered Energy Flows in Artificial Materials. *Phys. Rev. Lett.* **2002**, *89*, 186802-1−186802-4.
(31) Furuta, K.; Fujii, M.; Sugimoto, H.; Imakita, K. Energy Transfer in Silicon Nanocrystal Solids Made from All-Inorganic Colloidal Silicon Nanocrystals. *J. Phys. Chem. Lett.* **2015**, *6*, 2761−2766.
(32) Limpens, R.; Lesage, A.; Stallinga, P.; Poddubny, A. N.; Fujii, M.; Gregorkiewicz, T. Resonant Energy Transfer in Si Nanocrystal Solids. *J. Phys. Chem. C* **2015**, *119*, 19565−19570.
(33) Braun, M.; Tuffentsammer, W.; Wachtel, H.; Wolf, H. C. Tailoring of Energy Levels in Lead Chloride Based Layered Perovskites and Energy Transfer Between the Organic and Inorganic Planes. *Chem. Phys. Lett.* **1999**, *303*, 157−164.
(34) Yin, J.; Cortecchia, D.; Krishna, A.; Chen, S.; Mathews, N.; Grimsdale, C.; Soci, C. Interfacial Charge Transfer Anisotropy in

DOI: 10.1021/acs.jpcc.6b04768
J. Phys. Chem. C 2016, 120, 13310−13315

Polycrystalline Lead Iodide Perovskite Films. *J. Phys. Chem. Lett.* **2015**, *6*, 1396−1402.
(35) Ning, Z.; Gong, X.; Comin, R.; Walters, G.; Fan, F.; Voznyy, O.; Yassitepe, A. B.; Hoogland, S.; Sargent, E. H. Quantum-Dot-in-Perovskite Solids. *Nature* **2015**, *523*, 324−328.
(36) Swarnkar, A.; Chulliyil, R.; Ravi, V. K.; Irfanullah, M.; Chowdhury, A.; Nag, A. Colloidal $CsPbBr_3$ Perovskite Nanocrystals: Luminescence beyond Traditional Quantum Dots. *Angew. Chem., Int. Ed.* **2015**, *54*, 15424−15428.
(37) Pankove, J. I. *Optical Processes in Semiconductors*; Dover: New York, 1971.
(38) Lakowicz, J. R. *Principles of Fluorescence Spectroscopy*; Springer: New York, 2006.
(39) De Vries, P.; van Coevorden, D. V.; Lagendijk, A. Point Scatterers for Classical Waves. *Rev. Mod. Phys.* **1998**, *70*, 447−466.
(40) Delerue, C.; Lannoo, M. *Nanostructures: Theory and Modelling*; Springer-Verlag: Berlin, 2004.
(41) De Roo, J.; Ibanez, M.; Geiregat, P.; Nedelcu, G.; Walravens, W.; Maes, J.; Martins, J. C.; van Driessche, I.; Kovalenko, M. V.; Hens, Z. Highly Dynamic Ligand Binding and Light Absorption Coefficient of Cesium Lead Bromide Perovskite Nanocrystals. *ACS Nano* **2016**, *10*, 2071−2081.
(42) Efros, A. L.; Rosen, M.; Kuno, M.; Nirmal, M.; Norris, D. J.; Bawendi, M. Band-Edge Exciton in Quantum Dots of Semiconductors with a Degenerate Valence Band: Dark and Bright Exciton States. *Phys. Rev. B: Condens. Matter Mater. Phys.* **1996**, *54*, 4843−4857.
(43) Sun, Q.; Wang, Y. A.; Li, L. S.; Wang, D.; Zhu, T.; Xu, J.; Yang, C.; Li, Y. Bright Multicolored Light-Emitting Diodes Based on Quantum Dots. *Nat. Photonics* **2007**, *1*, 717−722.
(44) Zhao, J.; Bardecker, J. A.; Munro, A. M.; Liu, M. S.; Niu, Y.; Ding, I. K.; Luo, J.; Chen, B.; Jen, A. K. Y.; Ginger, D. S. Efficient CdSe/CdS Quantum Dot Light-Emitting Diodes Using a Thermally Polymerized Hole Transport Layer. *Nano Lett.* **2006**, *6*, 463−467.
(45) Mayilo, S.; Hilhorst, J.; Susha, A. S.; Höhl, C.; Franzl, T.; Klar, T. A.; Rogach, A. L.; Feldmann, J. Energy Transfer in Solution-Based Clusters of CdTe Nanocrystals Electrostatically Bound by Calcium Ions. *J. Phys. Chem. C* **2008**, *112*, 14589−14594.
(46) Valenta, J. Determination of Absolute Quantum Yields of Luminescing Nanomaterials Over a Broad Spectral Range: From the Integrating Sphere Theory to the Correct Methodology. *Nanosci. Methods* **2014**, *3*, 11−27.

DOI: 10.1021/acs.jpcc.6b04768
J. Phys. Chem. C 2016, 120, 13310−13315